Available online at www.sciencedirect.com
ScienceDirect
Building and Environment 42 (2007) 1994–2003
BUILDING AND ENVIRONMENT
www.elsevier.com/locate/buildenv

Numerical modelling as a tool for optimisation of sub-slab depressurisation systems design

Martin Jiranek, Zbynek Svoboda*

Faculty of Civil Engineering, Czech Technical University, Thakurova 7, 166 29 Prague, Czech Republic

Received 21 March 2003; received in revised form 10 October 2004; accepted 11 April 2006

Abstract

The following paper is focused on possibilities of a numerical modelling of sub-slab depressurisation systems, which belong among the most effective radon protective measures. Three recently developed computer programs are briefly described in the paper—mainly from the point of view of governing equations and basic numerical analysis approach. The paper also presents results of sensitivity tests for these numerical models. In addition, a comparison of numerical simulation results with measured data is included as well.

Keywords: Sub-slab depressurisation systems; Radon; Air pressure; Temperature; Numerical analysis; Finite element method

1. Introduction

Sub-slab depressurisation systems (SSD systems) belong among the most effective radon protective and remedial measures. These systems are designed in order to decrease the air pressure beneath buildings and to reduce the radon concentration in the soil gas. The air pressure is reduced by means of fans, which draw the soil air from one or several sumps [1,2] or from perforated pipes drilled beneath existing floors [3,4]. The effectiveness of these systems—as well as the occurrence of various negative side effects—is influenced by several key factors, such as floor tightness, vertical profile of soil permeability, number of fans, individual fan power and location and size of sumps or pipes [4]. The numerical modelling can be used as a powerful tool in the design phase of such systems [5–8]. With the help of numerical methods, it is possible to investigate how the specific layout of the ventilation system affects its operation and efficiency.

The analyses, which are usually needed for the comprehensive assessment of the SSD systems functionality, include the calculation of air pressure and air flow velocity fields in the soil underneath the building and the estimation of radon concentration field in the soil gas. The calculation of the temperature field in the ground is also necessary in order to examine how the SSD systems influence the heat loss through the floor and the internal surface temperatures on all constructions adjacent to the ground.

It is usually possible to use the simplification of steady-state processes for all the calculations mentioned above. The following governing equations for these transport mechanisms are all valid with the assumption of the steady-state transfer.

2. Governing equations

2.1. Air pressure field

The multidimensional steady-state air pressure field in a porous medium can be calculated by means of the well-known partial differential equation

$$k \cdot \nabla^2 P = 0, \tag{1}$$

which can be used with the assumption that the air is incompressible and the air flow is laminar. Under the same conditions, the air flow velocity field can be calculated from Darcy's Law

$$\vec{v} = -\frac{k}{\mu} \nabla P. \tag{2}$$

*Corresponding author. Fax: +420 233 339 987.
E-mail address: svobodaz@fsv.cvut.cz (Z. Svoboda).

0360-1323/$ - see front matter © 2006 Elsevier Ltd. All rights reserved.
doi:10.1016/j.buildenv.2006.04.002

Nomenclature

a_{Ra}	mass activity of radium Ra^{226} in material (Bq/kg)
b	thickness of transfer layer (m)
C	radon concentration in soil gas (Bq/m^3)
C_a	radon concentration in ambient air (Bq/m^3)
c_a	thermal capacity of air (1010 J/kg K)
D_e	effective radon diffusion coefficient (m^2/s)
D_0	radon diffusion coefficient in air (1.1×10^{-5} m^2/s)
f	radon emanation coefficient (dimensionless)
G	radon generation rate (Bq/m^3 s)
h_r	radon transfer coefficient (m/s)
k	permeability of porous medium (m^2)
P	air pressure (Pa)
$\vec{v}$	air flow velocity (m/s)
v_n	velocity component normal to boundary (m/s)
ε	porosity (dimensionless)
λ	thermal conductivity (W/m K)
λ_r	radon decay constant (2.1×10^{-6} 1/s)
μ	dynamic viscosity of air (1.7×10^{-5} kg/m s)
θ	temperature (°C)
ρ	bulk density of material (kg/m^3)
ρ_a	air density (1.2 kg/m^3)
$\partial/\partial n$	derivative in the direction of external normal to the boundary

The second assumption introduced above is satisfied if the relevant Reynolds number does not exceed the dividing line between the laminar and turbulent air flow which is for the porous materials shifted significantly lower than it is usual for the fluid flow in pipes. Deviations from Darcy's Law can be detected according to various researchers for Reynolds number reaching the limit value in the range from 1 to 70 [7,9,10]. If we consider the limit Reynolds number rather conservative value of 5, it is possible to calculate that such low Reynolds number is typical for all building materials with permeability lower than 10^{-8} m^2 (if the pressure gradient does not exceed 50 Pa). Most building materials and types of soil have such low permeability and so the laminar air flow through them is usually guaranteed if pressure gradients are not higher than 50 Pa. Nevertheless, the control of Reynolds number after the calculation of velocity field is essential.

The numerical solution of Eqs. (1) and (2) causes no major problems and can be found in several publications, e.g. [12,13].

2.2. Temperature field

The heat transfer in the soil region with an SSD system cannot be taken as a simple heat conduction. The heat transfer caused by convection is also very important in this case and thus the combined heat transfer must be taken into account. The partial differential equation governing this process can be expressed as

$$\lambda \nabla^2 \theta - \vec{v} \cdot \rho_a \cdot c_a \cdot \nabla \theta = 0. \tag{3}$$

Eq. (3) belongs to the family of convective-diffusion equations. Its numerical solution can be derived with the same assumptions as the solution of Eq. (1). The natural convection of air in the soil can be simultaneously neglected because the pressure difference caused by fans is the prevailing factor. With these assumptions and simplifications implemented, it is possible to derive the finite element method (FEM) solution of Eq. (3) by means of Petrov–Galerkin process. Detailed discussion of this approach including numerical stability analysis can be found in several previously published papers [14,15].

2.3. Radon concentration field

The distribution of radon concentration in the soil underneath a building is governed by another type of convective-diffusion equation. This differential equation can be written as

$$D_e \nabla^2 C - \frac{\vec{v}}{\varepsilon} \nabla C + G - \lambda_r C = 0. \tag{4}$$

with the radon generation rate defined as

$$G = \frac{a_{Ra} \cdot \lambda_r \cdot \rho \cdot f}{\varepsilon}. \tag{5}$$

The first term on the left-hand side of Eq. (4) represents the radon transport due to diffusion; the second term represents the radon transport due to convection. The third term expresses the increase of radon concentration due to radon generation rate in the soil or material pores and the last term represents the drop in radon concentration due to its radioactive decay. The radon transport caused by water flow is neglected in Eq. (4) due to its minor importance. The validity of Eq. (4) is conditioned by the same assumptions as the validity of Eq. (3).

Interesting issue is the definition of boundary conditions for Eq. (4). In most of the cases, two simple types of Dirichlet boundary condition are used. The first type is defined for the boundary between the soil and the air as

$$C = C_a, \tag{6}$$

and the second type for deep layers of the soil as

$$C = \frac{G}{\lambda_r}. \tag{7}$$

The main problem of easy-to-use Dirichlet boundary condition is in the fact that this condition directly defines the radon concentrations on the boundaries of the calculated area. This approach does not lead to substantial errors in the radon concentration field in the soil, but on

the other hand the error in estimation of the radon exhalation rate from the soil could be considerably high. The measurements show that the radon concentration right on the surface of radon-productive soil or floor is always higher than the radon concentration in the ambient air. Thus, if the radon concentration in the air is taken as the radon concentration on the soil or floor surface, the radon exhalation rate from the soil or floor is underestimated. This can be even dangerous in the case of evaluation of radon protective measures. In such cases, Newton type of boundary condition should be used—preferably in the following form:

$$-\varepsilon \cdot D_e \frac{\partial C}{\partial n} + v_n \cdot C = h_r \cdot (C - C_a) \tag{8}$$

with the radon transfer coefficient h_r defined as

$$h_r = \frac{D_0}{b}. \tag{9}$$

The thickness of the transfer layer b can be calculated according to Nemec [16] as

$$b = \sqrt{\frac{D_0}{\lambda_r}} \cdot \frac{\varepsilon \cdot D_e}{D_0}, \tag{10}$$

with the values of ε and D_e characterising the top-most layer of the soil or the floor.

With the use of Newton boundary condition (8), it is possible to calculate more exactly the radon concentrations on the soil and floor surfaces and subsequently also the radon exhalation rates.

The FEM solution of Eq. (4) can be derived by means of the Petrov–Galerkin approach again. More details of this derivation process and discussion on the numerical stability of its results can be found in [5].

3. Sensitivity analysis and verification of models

The reliability of recently developed computer programs Press3D, Wind2D and Radon2D (all based on the FEM solution of Eqs. (1), (3) and (4)) was tested on several soil profiles and several houses with different types of sub-slab depressurisation systems [17]. In the following part of this article, the sensitivity analysis of these numerical models is presented. Since the results of SSD systems sensitivity analysis are always closely connected to the house geometry used in calculations, they cannot be usually generalised and must be provided for a particular house. The whole process is illustrated on a single-family house located in Milesov, Czech Republic. The comparison of the calculated and measured values of underpressure, temperature and radon concentration in the soil gas is also included.

3.1. Experimental house and its numerical model

The chosen house is around 100 years old and has three habitable rooms in the ground floor (Fig. 1). The initial mean indoor radon concentration in the house was 1550 Bq/m^3. The remediation of the house was based on the installation of the SSD system in combination with the reconstruction of floors (old concrete floor slabs were replaced by the new ones, 50 mm thick thermal insulation was added). Perforated pipes were laid directly to the drainage layer of highly permeable gravel. The layout and diameters of pipes can be seen in Fig. 1. Perforated pipes were connected to the vertical exhaust pipe, which was inserted into a free flue and ended with a roof fan above the chimney.

The geometry of the house and the adjacent soil used in the numerical model was derived from the plan of the house and from the layout of pipes (Fig. 1). The circular pipes were replaced in the model by the pipes with a square cross-section. Pressure loss due to friction in the pipes was incorporated to the calculation in a simplified way by means of their permeability ($k = 3 \times 10^{-8}$ m^2). The soil under the house was modelled as a large block reaching in the horizontal direction 1 m beyond the perimeter walls. The depth of this block was taken as 3 m (Fig. 2). In accordance with the site investigation, two soil layers of

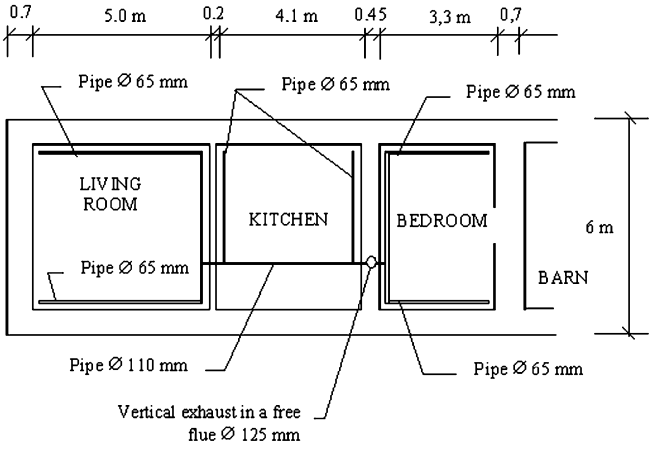

Fig. 1. Layout of perforated pipes in the experimental house.

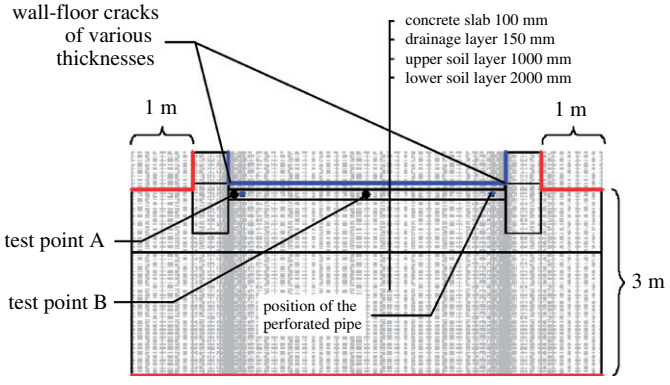

Fig. 2. Cross-section of the model (through the living room) with FEM mesh and boundary conditions for calculation of 2D radon concentration field.

Table 1
Material characteristics used in the numerical simulation as constant values

Material	Perme-ability k (m^2)	Porosity ε (dimensionless)	Effective radon diffusion coefficient D_e (m^2/s)	Radon generation rate G ($kBq/m^3 s$)	Thermal conductivity λ (W/m K)
Drainage layer	1×10^{-9}	0.30	9×10^{-6}	—	1.2
Concrete constructions	1×10^{-16}	0.10	1×10^{-8}	—	1.5

different permeability were considered. The dimensions of the floor slab and foundations were taken in compliance with the real house.

3.2. Sensitivity analysis

Only such parameters that can significantly influence the monitored quantities were varied in the sensitivity analysis of the model. Parameters with minor importance (e.g. characteristics of concrete structures) and parameters measured with a sufficient accuracy (e.g. the permeability of the drainage layer and the underpressure at the bottom of the vertical exhaust pipe) were taken as constant values. Their overview can be found in Table 1. The boundary conditions used in the calculations were defined as close to mean values of measured data as it was possible. A summary of applied boundary conditions is presented in Table 2.

The results of the sensitivity analysis are summarised in Table 3. The variations of various parameters used in the analysis were chosen in order to include typical ranges of material properties in the calculations. All the results are valid for the concrete floor slab with cracks of various widths around its perimeter.

The results show clearly that in real conditions (i.e. when cracks occur in the house sub-structure) the values of monitored quantities are influenced mainly by the technical state of the building sub-structure and by the performance of the sub-slab depressurisation.

The underpressure in the drainage layer under the house depends mainly on the leakage area, the indoor/sub-soil pressure difference and the underpressure generated in drainage pipes due to the soil ventilation. The soil permeability becomes an important parameter for the leakage area lower than $0.01\,m^2$. Vertical profile of soil permeability should be considered, if there is no air flow from the soil into the house through the structures in contact with the soil (Fig. 3).

The radon concentration in the drainage layer is not uniform and therefore it was necessary to define two different points, in which radon concentrations were studied. The point A was located under the wall-floor crack and the point B under the centre of the living room. Whilst the concentration at the point A indicates modifications in the radon supply rate, the concentration at the point B shows effectiveness of the soil ventilation.

Table 2
Boundary conditions used in calculations

Parameter	Position of the boundary condition			
	Soil surface	Floor surface	Deep soil	Exhaust pipe
Relative pressure (Pa)	Various values—see Table 3		−6	−65
Radon concentration (kBq/m^3)	0.01	0.10	57	—
Radon transfer coefficient (m/s)	18×10^{-5}	53×10^{-3}	10 000	—
Temperature (°C)	5	22	5	—
Heat transfer coefficient ($W/m^2 K$)	23	6	10 000	—

The radon concentration at the point A is influenced very strongly by the leakage area and by the indoor/sub-soil pressure difference (Fig. 4). On the other hand, these parameters have no effect on the concentration at the point B.

The influence of the soil permeability on the radon concentration at the point A increases with the reduction of the leakage area in the floor slab. The importance of the soil permeability at the point B is dependent on the radon generation rate (Fig. 5), which plays here a far more significant role than at the point A. The soil porosity and the radon diffusion coefficient in the sub-soil can be considered as negligible parameters, because they cause smaller changes in radon concentrations than 10%.

The changes induced by variations of input data in the values of the last monitored quantity—the sub-slab temperature—are rather minor in comparison with the changes in the values of radon concentration and underpressure. In accordance with expectations, the temperatures in the sub-slab area depend mainly on the quality of the used thermal insulation. However, the observed changes are not higher than 10% for the usual range of the thermal conductivity of common thermal insulations.

Other factors, such as the soil permeability and the indoor/sub-soil pressure difference, have almost negligible effect on the temperature. The leakage area is more relevant—especially in the case of the sub-slab area close to the cracks (test point A). Nevertheless, even in this case the increase of the temperature in this region is not higher than 7% for the common width and number of cracks.

Table 3
Results of the sensitivity analysis including variations of input parameters

Monitored quantity	Part of the model	Material parameter or boundary condition	Unit	Variations (from lower limit to upper limit)	Modification of the monitored quantity due to the change of the relevant parameter (from lower to upper limit)	
					Test point A	Test point B
Radon concentration in the drainage layer in depth of 50 mm under the slab	Subsoil 0–3 m	Porosity	(dimensionless)	0.2–0.4	−10%	−10%
		Rn diffusion coefficient	(m^2/s)	5×10^{-7}–2×10^{-6}	+10%	+5%
		Rn generation rate	Bq/(m^3 s)	0.2–0.4	+(20–30)%[a]	+(60–95)%[b]
		Soil permeability	(m^2)	1×10^{-13}–1×10^{-11}	+(25–270) %[c]	+(45–80)%[d]
	Concrete slab	Total leakage area	(m^2)	0.05–0.01	+(1600–3500)%[a]	±0%
	Floor surface	Relative pressure	(Pa)	0 to −4	$+2\times10^4$%	±0%
	Soil surface	Relative pressure	(Pa)	−2 to +2	±0%	±0%
Underpressure in the drainage layer in depth of 50 mm under the slab	Subsoil 0–3 m	Soil permeability	(m^2)	1×10^{-13}–1×10^{-11}	—	−(15–85)%[e]
	Concrete slab	Total leakage area	(m^2)	0.05–0.0025	—	+(252–486)%[b]
				0 to 0.05	—	−(560–2800)%[b]
	Floor surface	Relative pressure	(Pa)	0 to −4	—	+3700%
	Soil surface	Relative pressure	(Pa)	−2 to +2	—	±0%
Temperature in the drainage layer in depth of 50 mm under the slab	Subsoil 0–3 m	Soil permeability	(m^2)	1×10^{-13}–1×10^{-11}	±0%	±0%
	Concrete slab	Leakage area	(m^2)	0–0.05	+7%	+1%
	Thermal insulation	Thermal conductivity	(W/m K)	0.035–0.050	+3%	+10%
	Floor surface	Relative pressure	(Pa)	0 to −4	−2%	±0%
	Soil surface	Relative pressure	(Pa)	−2 to +2	−2%	±0%

[a]Higher value corresponds to higher soil permeability.
[b]Higher value corresponds to lower soil permeability.
[c]Lower value is valid for the leakage area of 0.05 m^2 and higher value for the leakage area of 0.01 m^2.
[d]Higher value corresponds to lower radon generation rate.
[e]Lower value is valid for the leakage area of 0.05 m^2 and higher value for the slab without cracks.

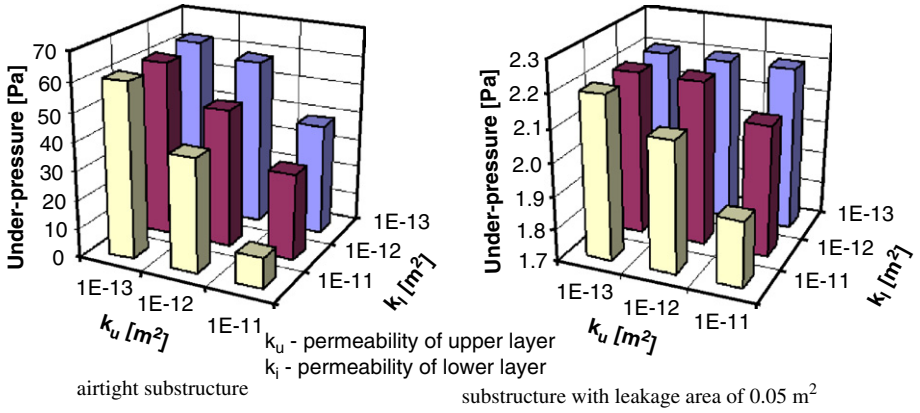

Fig. 3. Influence of variations of the soil permeability on the sub-floor underpressure (test point B).

Presented results of the sensitivity analysis are related to the particular house, its geometry and the type of the sub-slab depressurisation system and cannot be generalised. Different arrangement of the soil ventilation and different properties of the house sub-structure can lead to quite different conclusions.

3.3. Comparison of measured and calculated values

In general, a reliable verification of any numerical model by comparison with measured data is possible only with the input parameters as close to measured values as feasible. Therefore, a thorough investigation of the sub-soil and the

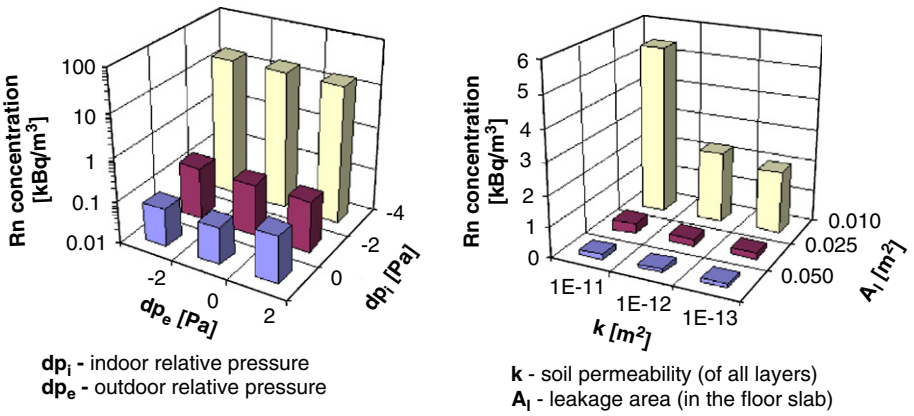

Fig. 4. Influence of variations of the leakage area and the pressure difference on radon concentrations (test point A).

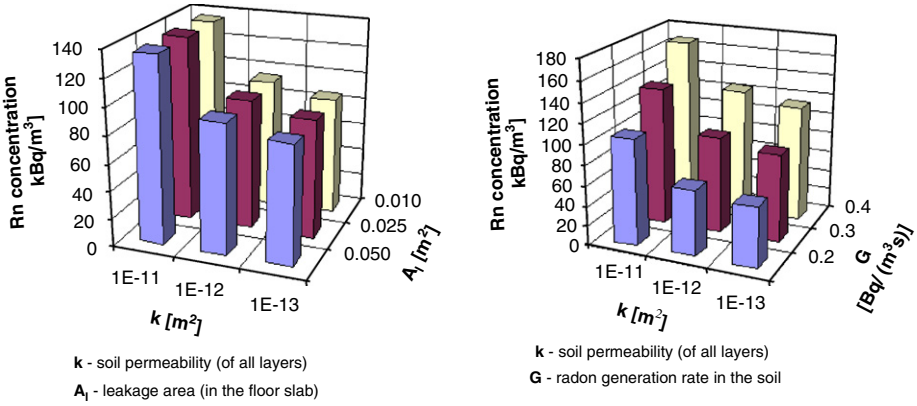

Fig. 5. Influence of variations of the leakage area, the soil permeability and the radon generation rate in the soil on radon concentrations (test point B).

experimental single-family house in Milesov was performed in order to obtain all necessary data.

During the measurements, the house was in ordinary use by the owner's family. Soil air temperatures and indoor/outdoor and indoor/sub-floor pressure differences were measured continuously. Simultaneously, the indoor air temperature, indoor radon concentration and outdoor air temperature were also registered. All measurements were carried out for both possible cases: for the period with the SSD system switched off and for the period with the SSD system in operation.

A detailed building survey focused on the air-tightness of the floors in contact with the soil was performed in order to assess the leakage area. Based on this survey, 0.5 mm wide wall-floor cracks along both longitudinal perimeter walls were incorporated into the numerical simulation.

The investigation of the foundation soils included the measurement of the radon concentration in the soil gas in 15 points around the house (third quartile in the depth of 0.8 m was 57 kBq/m^3) and the assessment of the vertical profiles of the soil permeability and radon concentration in the soil air. Radon generation rate was estimated with respect to the measured vertical profile of the soil gas radon concentration so that the calculated profile corresponds to the measured one. Other material parameters such as radon diffusion coefficient, soil porosity and thermal conductivity were adopted from the database based on the survey of literature and technical standards. Material characteristics used in the numerical simulations are summarised in Table 4. All values of the input parameters, including the estimated uncertainties, are within the intervals used for the sensitivity analysis.

Boundary conditions were applied according to Table 2. At the bottom of the vertical exhaust pipe, the measured underpressure of −65 Pa was considered. The indoor relative pressure was chosen as −2 Pa in the calculations, while the outdoor relative pressure was considered to be 0 Pa. Both values were based on the measurement results and corresponded to the mean values of measured relative pressures.

The three-dimensional air pressure field in the whole sub-slab space of the experimental house was calculated by means of the computer program Press3D. The results of the air pressure field calculation for the case of fan in

Table 4
Material characteristics used in numerical simulation

Measured material	Permeability (m^2)	Porosity (dimensionless)	Radon diffusion coefficient (m^2/s)	Radon generation rate ($kBq/m^3 s$)	Thermal conductivity (W/m K)
Concrete floor construction	1.0×10^{-16}	0.10	1×10^{-8}	—	1.50
Concrete foundations	1.0×10^{-16}	0.10	1×10^{-8}	—	2.10
Thermal insulation	1.0×10^{-14}	0.30	1×10^{-7}	—	0.04
Soil in the depth from 0 to 1 m	1.5×10^{-12}	0.30	1×10^{-6}	1.0×10^{-4}	1.90
Soil in the depth from 1 to 3 m	1.0×10^{-11}	0.30	2×10^{-6}	1.2×10^{-4}	2.00

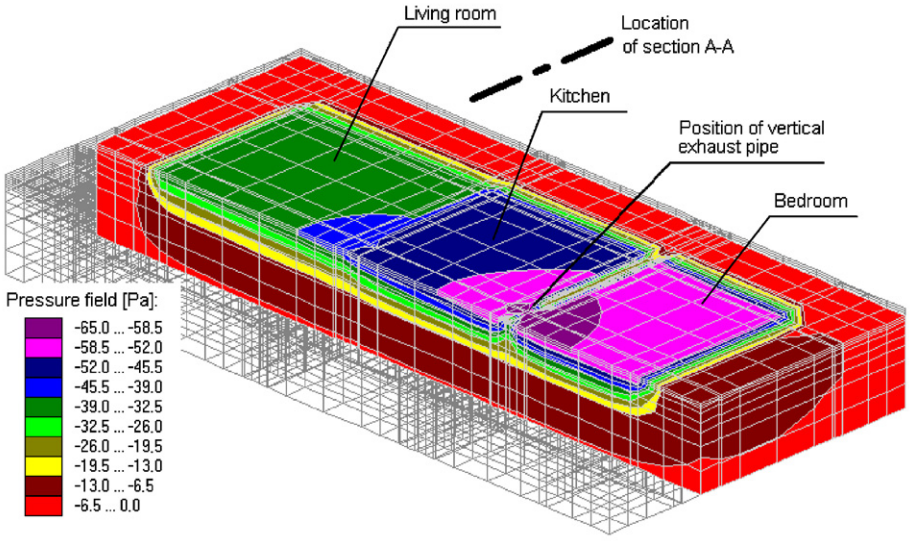

Fig. 6. Three-dimensional view of the calculated pressure field in the sub-slab space of the experimental house (cut-out).

operation (with underpressure of −65 Pa in the exhaust pipe) are shown in Figs. 6 and 7. The test points are also marked in the same figures together with the measured values of underpressure for the considered boundary conditions. It can be seen that the correlation between calculated and measured values is very good—differences are not higher than 10%.

The two-dimensional steady-state temperature field in the soil under the experimental house was calculated by means of the program Wind2D. The calculation of the temperature field was carried out twice—once for the case with the SSD system in operation and once for the case with the fan switched off. Results of the calculation for the non-ventilated soil can be seen in Fig. 8 and for the ventilated soil in Fig. 9. Both figures represent the cross-section A-A through the sub-slab region under the living room. For the working cycle, the temperature distribution was determined using the mean underpressure of −37 Pa as the boundary condition in the perforated pipes located in the drainage layer. This value was derived from the results of the three-dimensional pressure field calculation (see Fig. 7) and was also compared with the measured values in order to reach a good agreement with the experimental data. All other boundary conditions were taken according to Table 2.

The test points, where the temperatures were measured in situ, are marked again by the black dots in Figs. 8 and 9. It can be seen from both figures that the differences between measured and calculated values are up to 15%. The calculation results as well as the measured data show very clearly the effect of the soil ventilation on the sub-floor temperatures. If the soil is ventilated by continuously operating fans, the decrease of the temperatures under the floor slab with 50 mm thick thermal insulation can be as high as 2 °C. The theoretical model shows also—in the same way as the measured data do—the negative effect of thermal bridges on the perimeter of the house (uninsulated foundations). The temperatures in the drainage layer in the vicinity of perimeter walls are approximately 1 °C lower than those in the same layer in the middle of the house.

Finally, the two-dimensional steady-state field of radon concentrations in the soil under the experimental house was calculated by means of the FEM program Radon2D.

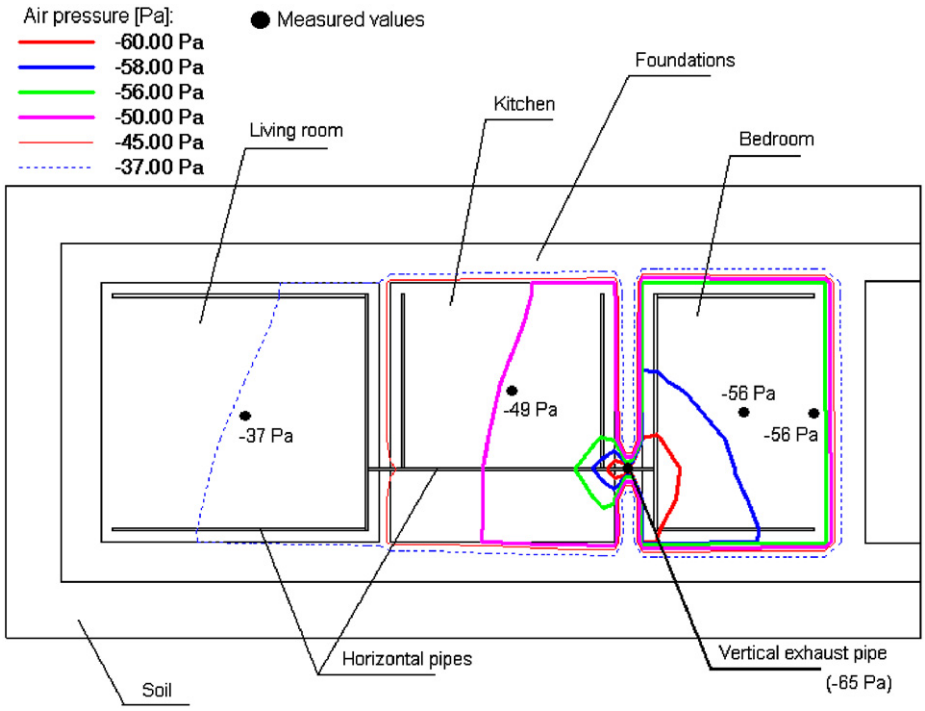

Fig. 7. Two-dimensional view of the calculated pressure field in the drainage layer.

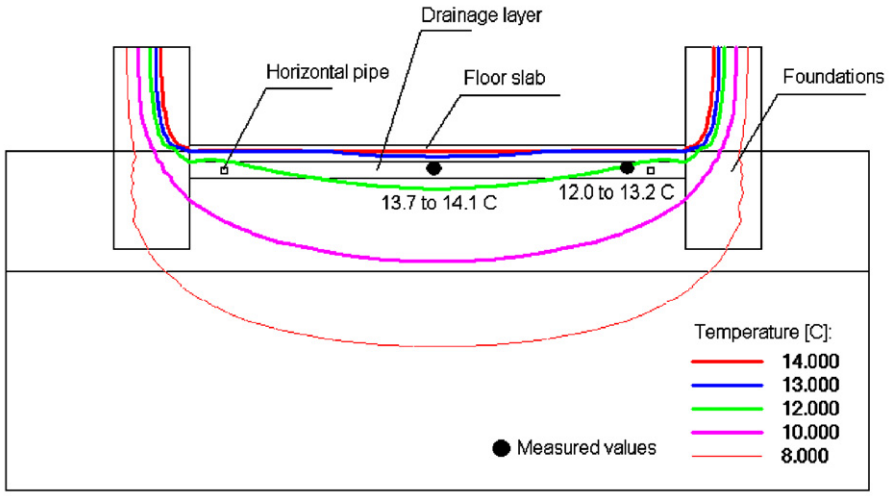

Fig. 8. Calculated temperature distribution in the sub-slab region—SSD system out of operation.

The underpressure in the perforated pipes was introduced in the calculation exactly in the same way as in the case of temperature field calculation. Another similarity between these two calculations is in the fact that both were carried out twice—for the ventilated and for the non-ventilated soil. The results of the radon concentration field assessment are presented in Figs. 10 and 11. The correlation between measured and calculated values of the radon concentration is worse than in the cases of the temperature and air pressure fields—differences range from 20%–85%. Nevertheless, the trends in the radon concentration distribution are simulated in the numerical model with a sufficient reliability. The calculation results show for example that the soil ventilation can induce the reduction of the radon concentration in the drainage layer from the mean value of 23 kBq/m^3 (SSD system switched off) to the mean value of 14 kBq/m^3 (SSD system in use). This result corresponds with the general trends obtained from the measurement.

4. Conclusion

The radon concentration and the pressure distribution in the drainage layer under the houses with SSD systems are influenced mainly by the degree of the air-tightness of the

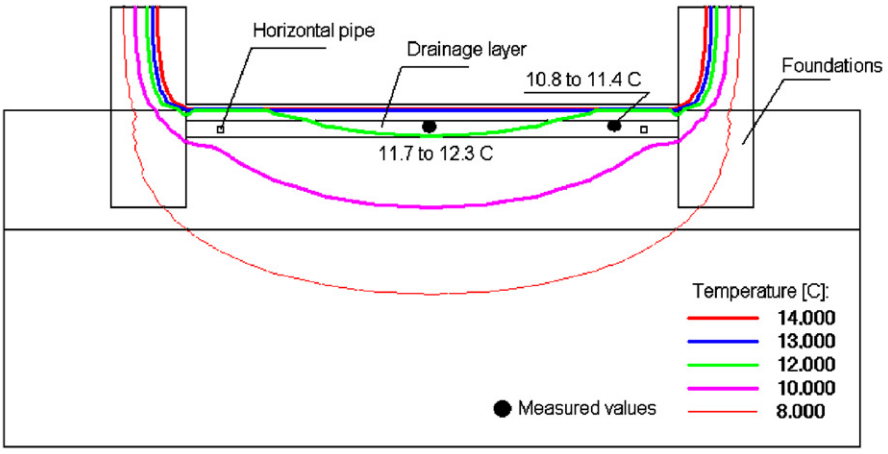

Fig. 9. Calculated temperature distribution in the sub-slab region—SSD system in use.

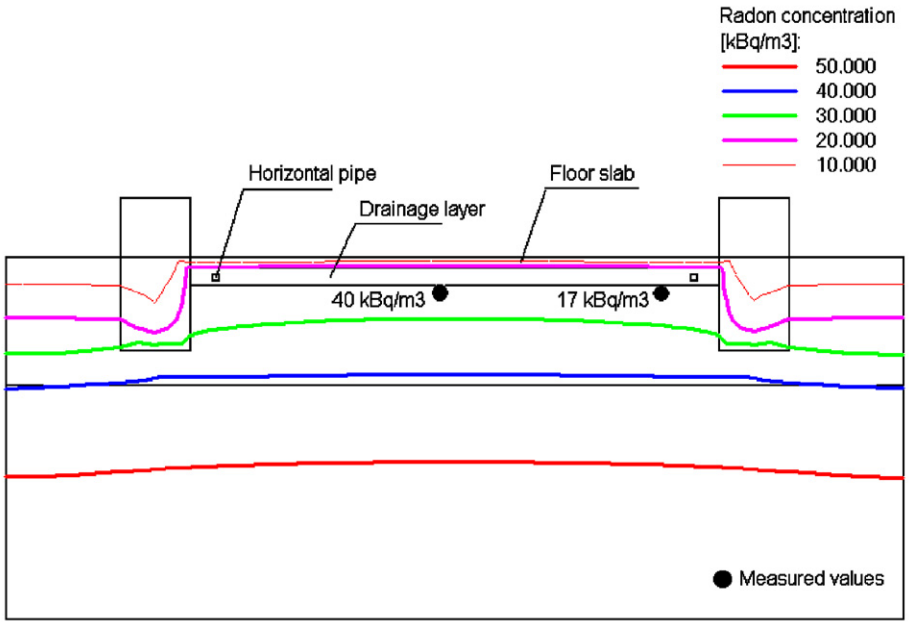

Fig. 10. Calculated radon concentration field in the sub-slab region—SSD system out of operation.

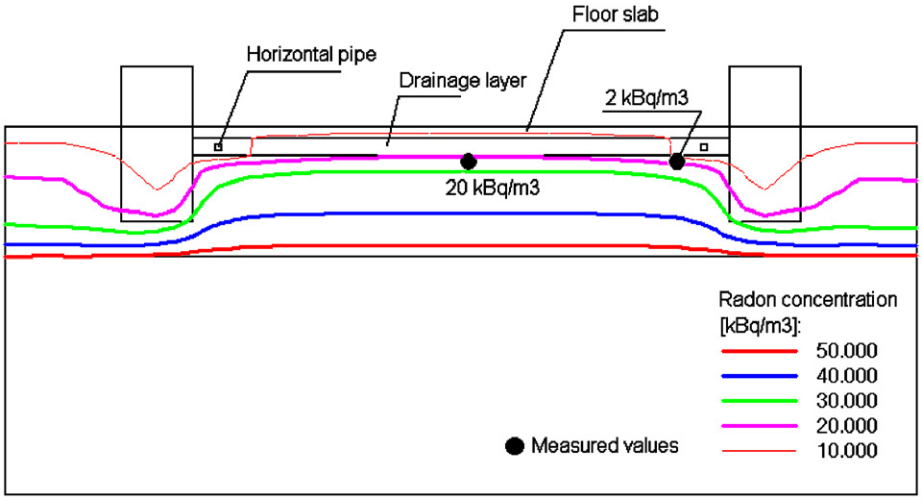

Fig. 11. Calculated radon concentration field in the sub-slab region—SSD system in use.

house structures in contact with the soil, by the indoor/sub-floor pressure differences and by the underpressure induced by the sub-slab depressurisation. As far as the sub-soil properties are concerned, only the permeability and the radon generation rate have significant influence on the accuracy of the numerical modelling.

Reliable inputs for the numerical modelling should be based on a thorough investigation of the particular building and its foundation soils. The leakage area in the floor slab can be estimated with the help of a blower-door test [18]. No problems usually occur with the assessment of pressure differences and permeabilities of soil layers, which can be measured relatively easily. The radon generation rate can be derived with a sufficient degree of accuracy from the measured vertical profile of the radon concentration in the soil gas.

Presented paper shows some possibilities of the numerical simulations in the field of radon protective measures. It has been confirmed by means of the verification based on experimental data that the developed numerical models can be used as effective tools for optimisation of SSD systems and for the prediction of occurrence of various negative side effects (e.g. the increase of the heat loss via the ground).

Acknowledgements

This paper has been supported by the Research Project MSM 6840770005.

References

[1] Clavensjo B, Akerblom G. The radon book Measures against radon. Stockholm: The Swedish Council for Building Research; 1994.

[2] Radon Sumps: a B.R.E. Guide to radon remedial measures in existing dwellings. Watford: Building Research Establishment; 1992.

[3] Jiranek M, Neznal M. Czech experience with sub-slab depressurisation systems. In: Radon investigations in the Czech Republic, Vol. VII. Prague; 1998. p. 119–24.

[4] Jiranek M. Efficiency and side effects of sub-slab depressurisation systems. In: Radon investigations in the Czech Republic, vol. IX. Prague; 2002. p. 87–94.

[5] Jiranek M, Svoboda Z. Verification of radon protective measures by means of a computer model. In: Proceedings of the fifth International IBPSA building simulation conference, vol. II, Prague; 1997: p. 165–72.

[6] Jiranek M, Svoboda Z. The computer model for simulation of soil ventilation systems performance. In: Proceedings of the European conference on protection against radon at home and at work, Prague; 1997. p. 110–3.

[7] Bonnefous YC, Gadgil AJ, Fisk WJ, Prill JR, Nematollahl AR. Field study and numerical simulation of sub-slab ventilation systems. Environmental Science and Technology 1992;26:1752–9.

[8] Andersen CE, Albarracin D, Csige I, Graaf ER, Jiranek M, Rehs B, Svoboda Z, Toro L. ERRICCA radon model intercomparison exercise. Roskilde: Riso National Laboratory; 1999.

[9] Gadgil AJ, Bonnefous YC, Fisk WJ. Relative effectiveness of sub-slab pressurisation and depressurisation systems for indoor radon mitigation—studies with an experimentally verified numerical model. Indoor Air 1994;4:265–75.

[10] Nazaroff WW, Sextro RG. Technique for measuring the indoor ^{222}Rn source potential in soil. Environmental Science and Technology 1989;23:451–8.

[12] Zienkiewicz OC, Taylor RL. The finite element method, 4th Edition. London: McGraw-Hill; 1991.

[13] Huebner KH, Thornton EA. The finite element method for engineers. New York: Wiley; 1982.

[14] Svoboda Z. The convective-diffusion equation and its use in building physics. International Journal on Architectural Science 2000;1(2): 68–79.

[15] Svoboda Z. The analysis of the convective–conductive heat transfer in the building constructions. In: Proceedings of the sixth international IBPSA building simulation conference, vol. I, Kyoto; 1999. p. 329–35.

[16] Jiranek M, et al. Building constructions—radon protective measures. Prague: Czech Technical University Press; 2000 [in Czech].

[17] Jiranek M, Schreyer J. Applicability of sub-slab depressurisation systems beneath existing houses. Prague: The Final Research Report for the State Office for Nuclear Safety and the Ministry of Industry and Commerce; 2002 [in Czech].

[18] ISO 9972. Thermal insulation—determination of air-tightness—fan pressurization method. 1996.